

# Effects of the Preparation Conditions on Ethylene/Vinyl Acetate Membrane Morphology with the Use of Scanning Electron Microscopy

M. Sadeghi,<sup>1</sup> S. A. Mousavi,<sup>2</sup> M. Y. Motamed Hashemi,<sup>2</sup> M. Pourafshari Chenar,<sup>3</sup> R. Roosta Azad<sup>2</sup>

<sup>1</sup>Chemical Engineering Department, Faculty of Engineering, Tarbiat Modarres University, Tehran, Iran

<sup>2</sup>Department of Chemical and Petroleum Engineering, Sharif University of Technology, Tehran, Iran

<sup>3</sup>Chemical Engineering Department, Faculty of Engineering, Ferdowsi University of Mashhad, Mashhad, Iran

Received 16 July 2006; accepted 21 December 2006

DOI 10.1002/app.26353

Published online 14 May 2007 in Wiley InterScience (www.interscience.wiley.com).

**ABSTRACT:** In this research, the effects of preparation conditions, including the coagulation bath temperature, polymer solution composition, preliminary drying time, and thickness of cast polymeric films, on the morphology of ethylene/vinyl acetate copolymer membranes were investigated with scanning electron microscopy and nitrogen gas permeability tests. Flat sheet membranes were prepared through a thermal-wet phase-inversion method. Scanning electron microscopy pictures showed asymmetric structures for some of the membranes. It was also observed that the porosity of the membranes decreased with an increase in the temperature of the coagulation bath and the solvent

evaporation period. When the concentration of the polymer solution was increased from 5 to 12 wt %, the nucleation and growth of the solvent-rich phase replaced the nucleation and growth of the polymer-rich phase. With an increase in the thickness of the cast polymeric films, the number of macrovoids increased in the membranes. The nitrogen gas permeability of the developed membranes was in good agreement with the scanning electron microscopy results. © 2007 Wiley Periodicals, Inc. *J Appl Polym Sci* 105: 2683–2688, 2007

**Key words:** membranes; morphology

## INTRODUCTION

Compared with other technologies, membrane separation seems to be competitive for purification and concentration applications, especially in gas industries. This is primarily due to lower energy consumption and hence better economy of separation, possible continuous operation, the availability of a vast variety of membranes for different applications, and the possibility of straightforwardly scaling up the process.<sup>1</sup> Membranes can also be used in combination with traditional gas-separation methods to take advantage of both technologies for certain occasions in which neither process can achieve a proper result individually.<sup>2</sup>

Using asymmetric membranes having surface pore sizes in the range of 1–50 nm, the ultrafiltration process separates extremely small, suspended particles and dissolved macromolecules from fluids.<sup>3</sup> Because of its great importance, the study of the ultrafiltration process has become one of the top research areas in recent years.<sup>2–12</sup> Numerous investigations have been focused on studies of the effects of opera-

tional conditions on the membrane performance, industrial applications, and fouling as well as the modeling of the transport properties of ultrafiltration.<sup>3,4</sup> Some investigators have studied the preparation, morphology, and performance of inorganic and polymeric membranes.<sup>2,3,5–12</sup> However, polymeric membranes are the most useful membranes used in various industries, especially in ultrafiltration, nanofiltration, reverse osmosis, and gas separation, because they can have various functional groups and be easily modified chemically.<sup>6</sup> Therefore, a great deal of research has been devoted to developing new types of polymeric membranes in recent years.<sup>6–12</sup>

Polymeric membranes are generally prepared by the phase-inversion process. In this process, a homogeneous polymer solution is spread over a suitable support with a doctor blade and then immersed in a nonsolvent coagulation bath. After immersion, solvent and nonsolvent exchange occurs across the interface between the cast solution and coagulation media.<sup>1</sup> The precipitation path of membranes forming in a coagulation process of dry/wet or wet casting is governed by the thermodynamics and kinetics of the process. In turn, there are many factors that affect the thermodynamics and kinetics of phase-inversion processes, and many investigators<sup>13–16</sup> have attempted to correlate them with the morphol-

Correspondence to: M. Sadeghi (msadeghi@modares.ac.ir).

ogy and one or more properties of the resulting membrane. It is well known that membrane preparation conditions, such as the coagulation bath composition and polymer solution formulation, have considerable effects on the final membrane structure and properties. Moreover, the addition of some additives to the polymer solution or the coagulation bath can be useful for changing the membrane structure from symmetric to asymmetric. For example, Deshmukh and Li<sup>11</sup> reported that the addition of polyvinylpyrrolidone (PVP) and ethanol to a casting solution of polyvinylidene fluoride (PVDF) and a water coagulation bath can change the membrane morphology. Yang and Liu<sup>12</sup> used CaCl<sub>2</sub> and NaCl as additives in the casting solution and coagulation bath, respectively, in the preparation of polyacrylonitrile ultrafiltration membranes. In their investigation, the addition of NaCl decreased the permeability of the membranes. Chaturvedi et al.<sup>3</sup> found that the acidic/basic nature of additives affects the viscosity of the casting solution as well as the water permeation rate of the resultant ultrafiltration membranes.

The ethylene/vinyl acetate (EVA) copolymer has recently been used for membrane preparation in various applications.<sup>17,18</sup> Marais et al.<sup>17</sup> studied the transport of O<sub>2</sub> and CO<sub>2</sub> gases through EVA membranes with different vinyl acetate contents. Mousavi et al.<sup>18</sup> reported that EVA membranes demonstrate good potential for air-separation applications.

In this study, EVA membranes were prepared through a thermal-wet phase-inversion process. The effects of the casting solution concentration, the as-cast polymer solution thickness, coagulation bath temperature, and preliminary evaporation time on the morphology of the final membrane properties were investigated with scanning electron microscopy (SEM) and nitrogen gas permeation tests.

## EXPERIMENTAL

### Materials

EVA copolymers containing 28 or 18% vinyl acetate were provided by Asia Polymer Corp. (Kaohsiung, Taiwan) and Exxon Chemical Co. (Belgium), respectively. Commercial-grade tetrahydrofuran (THF) was used as the solvent. Distilled water with a conductivity of 10 μS was used as a precipitant. Nitrogen with 99.99% purity (Roham Gas Corp., Tehran, Iran) was used for the permeability measurements.

### Preparation of the membranes

Casting solutions of 5 or 12 wt % EVA in THF were prepared at 50°C under stirring for several hours. After degassing, the prepared polymer solutions were cast onto a glass plate at room temperature

and then transferred to a coagulation bath after 0, 10, or 20 s of solvent evaporation. The temperature of the water coagulation bath was controlled to be ice-cold, 19°C, 39°C, or 53°C. Phase inversion started immediately after the immersion of the cast film, and a thin polymeric film detached from the glass plate after a few minutes. After about 15 min, the separated film was spread onto filter paper and dried at room temperature. The actual thickness of the membranes was measured with a micrometer.

### Membrane characterization

The morphological behavior of the prepared membranes was studied with SEM. To confirm the results obtained from SEM, nitrogen gas permeability measurements were performed with an experimental setup described elsewhere.<sup>14</sup>

The nitrogen permeability of the cast films ( $P$ ) in barrers was calculated as follows:

$$P = \frac{Ql}{A\Delta p} 10^{10}$$

where  $Q$  is the steady-state permeation rate [cm<sup>3</sup>(STP)/s],  $l$  is the membrane thickness (cm),  $A$  is the permeation area of the film (cm<sup>2</sup>), and  $\Delta p$  is the pressure difference across the film (cmHg).

The nitrogen permeability measurements were applied to determine if the membranes had a dense or porous structure.

## RESULTS AND DISCUSSION

A number of porous EVA/THF-based polymeric membranes with two different casting solutions (5 or 12 wt % EVA in THF) were prepared. For each composition, films with different casting thicknesses (580 or 1015 μm) were cast onto a glass plate. The asymmetric structure of the membranes was examined with SEM.

The coagulation medium plays an important role in the formation of membranes by the phase-inversion process. In general, a fast coagulation rate results in large, fingerlike, cavity-like formations and hence a large amount of porosity, whereas a slow coagulation rate results in a porous, spongelike membrane structure with less porosity.<sup>19,20</sup>

The effect of the coagulation bath temperature on the cross-sectional structure of the prepared membranes from a 12 wt % EVA solution is shown for the cast film thickness of 1015 μm in Figure 1 and for the cast film thickness of 580 μm in Figure 2. Figure 1(a–c) shows the membranes coagulated at 19°C. Figure 1(a) clearly indicates the asymmetric structure of the membrane, that is, a dense layer supported by a spongy, porous sublayer. Contrary to most other

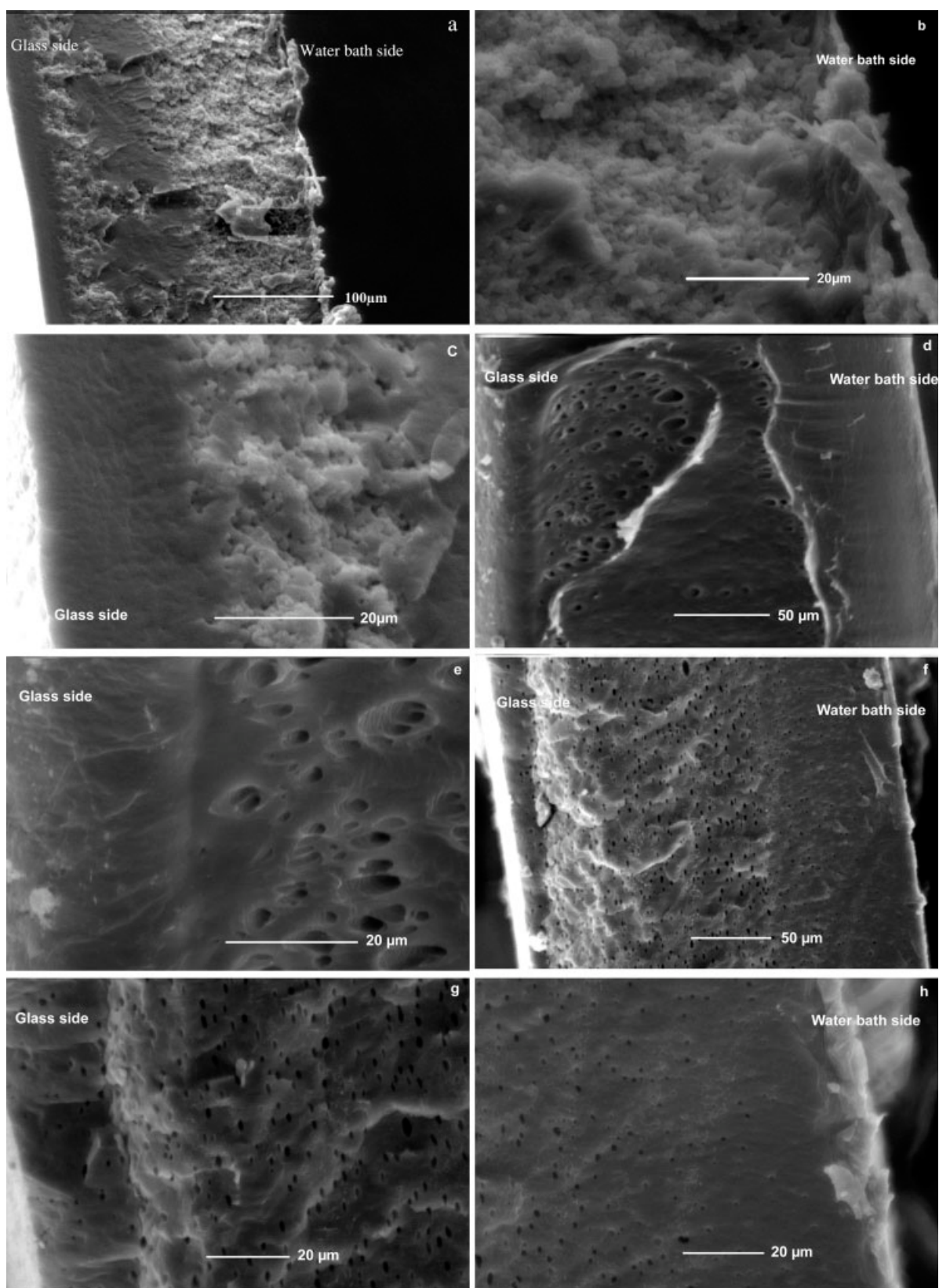


**Figure 1** Micrographs of EVA membranes cast from 12 wt % EVA/THF solutions at different coagulation bath temperatures (casting thickness = 1015  $\mu\text{m}$ , preliminary drying time = 10 s): (a) a cross-sectional view at 19°C, (b) a porous sub-layer of an integrally skinned porous membrane at 19°C, (c) an (almost) dense skin layer of a membrane on the glass side at 19°C, (d) a cross-sectional view at 39°C, (e) macrovoids and an (almost) dense skin layer on the glass side at 39°C, (f) a cross-sectional view at 53°C, (g) a membrane cross section on the glass side at 53°C, and (h) a membrane cross section on the coagulation bath side at 53°C.



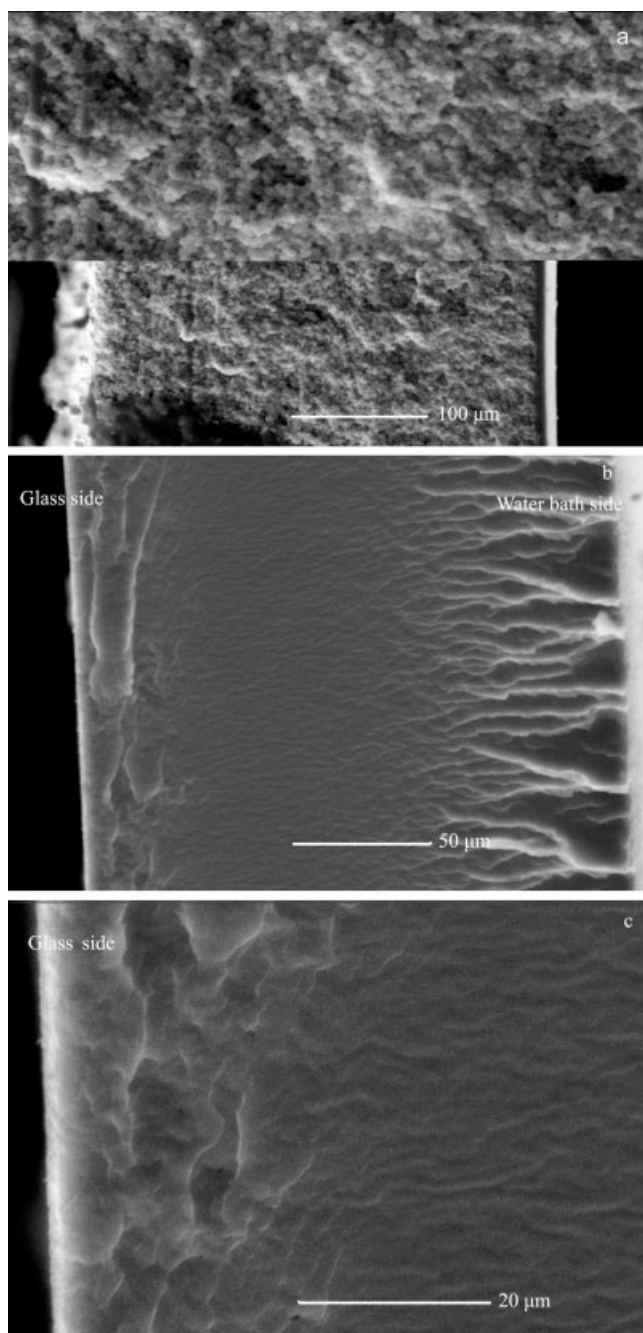


**Figure 2** Micrographs of EVA membranes cast from 12 wt % EVA/THF solutions at different coagulation bath temperatures (casting thickness = 580  $\mu\text{m}$ , preliminary drying time = 10 s): (a) a cross-sectional view at 4°C, (b) a cross-sectional view at 39°C, and (c) an (almost) dense skin layer on the glass side at 39°C.

membranes, the dense skin layer developed at the side that was in contact with the glass plate. This observation may be explained as follows.

Soon after the polymer solution is cast onto a glass plate, the gelation of the polymer takes place because of the sudden temperature decrease, and as a result, a relatively dense skin layer is formed on the glass side. When the cast solution film is brought into contact

with the coagulation media, the upper part of the film is subject to the immediate intrusion of water into the film because of the strong interaction between the water (coagulant) and THF (solvent). Hence, this side of the film becomes porous. As you go down to the bottom side (glass side), water/solvent exchange takes place more slowly because of the resistance of the dense layer that forms at the upper part of the film. Consequently, a porosity gradient is formed from the upper part to the lower part of the membrane. When the water/solvent exchange rate is increased, even the skin layer that forms on the glass side becomes more porous.<sup>19</sup> Figure 1(b,c) shows detailed views of the porous layer.

The structures of the polymeric films when coagulated at 39 and 53°C are shown in Figures 1(d,e) and 1(f–h), respectively. In these figures, the trapped macrovoids can be observed in dense polymeric membranes. These polymeric membranes contain some macrovoids trapped in the membrane structure. In other words, the spongy structure of Figure 1(a–c) turns into a denser structure when the coagulation temperature is increased from 19 to 39°C. Moreover, the size of the macrovoids trapped in the dense layer decreases from 7.31 to 2.45  $\mu\text{m}$  when the temperature is increased from 39 to 53°C. This may be explained as follows.

When the coagulation bath temperature reaches 19°C, an annealing process takes place simultaneously with the phase-inversion process. Annealing causes transitional motions of macromolecules that form the pore edges. These transitional motions bring the polymeric chain segments, on the same macromolecules or on the neighboring macromolecules, closer, and the polymers are virtually crosslinked. Thus, the membrane will shrink three-dimensionally, and the final structure of the membrane will have some macrovoids that are trapped in its structure.<sup>19</sup>

Higher coagulation bath temperatures increase the transitional motions of the polymer segments, and this will enhance the shrinkage, leading to a reduction of the size of the macrovoids. As a result of this phenomenon, membranes coagulated at higher temperatures (e.g., at 53°C) have a denser structure, as confirmed by nitrogen gas permeability experiments. Table I shows that the nitrogen gas permeability decreases from 126 to 68 barrer as the coagulation temperature increases from 39 to 53°C. Moreover, the nitrogen gas permeability corresponding to the coagulation bath temperature of 19°C is 33,015, which supports the more porous structure of this membrane shown in Figure 1(a–c). In accordance with these observations, the very high gas permeability of the films prepared at 19°C cancels out their ability to be applied in gas separation, but the membranes prepared at a higher temperature seem to be suitable for gas-separation applications.

**TABLE I**  
**Nitrogen Permeability Through EVA Membranes**  
**Coagulated at Different Temperatures**

Cast film thickness ( $\mu\text{m}$ )	Coagulation bath temperature ( $^{\circ}\text{C}$ )	Feed pressure (psig)	Permeability (barrer)
1015	19	10	33,015
1015	39	87	126
1015	53	87	68
580	4	10	39,383

As shown in Figure 1(c,e,g), the presence of a skin layer is evident, and because of the high polymer solution concentration, the skin layer is thick (ca. 20  $\mu\text{m}$  in all cases).

Figure 2(a) shows the structure of the thinner membrane coagulated at 4 $^{\circ}\text{C}$ . The membrane was cast from a 12 wt % EVA solution to a thickness of 580  $\mu\text{m}$ . The spongelike structure of the membrane is obvious. As shown in Table I, the nitrogen permeability is very high in this case, confirming the porous structure of the membrane. As expected, both the lower casting thickness and coagulation bath temperature enhanced the porosity of the prepared films. Figure 2(b,c) shows the structure of the membrane that coagulated at 39 $^{\circ}\text{C}$ . A thick and dense skin layer can be observed. These figures also support the earlier conclusion that an increase in the coagulation temperature leads to the formation of denser layers.

No macrovoids are captured in the dense skin layer shown in Figure 2(b,c). The thickness of the membrane is one-half of the membrane shown in Figure 1. Most likely, nuclei of the dilute phase have migrated quickly to the gelation media/polymer film interface and eventually escaped into the coagulation bath. The fingerlike structure observed at the right-hand side (coagulation media/polymer film interface) of Figure 2(b) probably shows the migration paths of the dilute phase. On the other hand, the nuclei of the dilute phase cannot escape from a thicker film but are trapped, forming macrovoids. This is evidenced by the pictures shown in Figure 1(e,g).

The presence of an evaporation step before the immersion of the membrane into a coagulation bath results in slower precipitation and the formation of a denser structure with a dense skin layer.

Figure 3(a–c) shows the effect of the evaporation period before the cast film was immersed into the coagulation bath. The membranes were cast from a 5 wt % EVA solution to a thickness of 580  $\mu\text{m}$ , and the coagulation bath temperature was 19 $^{\circ}\text{C}$ . The EVA concentration was much lower than that of the membranes shown in Figures 1 and 2. When a membrane is cast from a solution of such a low polymer concentration, the continuous phase will be the dilute

phase, in which the polymer-rich phase is dispersed. This is evidenced by the many polymeric particles observed in Figure 3. Hence, the nucleation and growth of the polymer-rich phase will govern the structure of the membranes ultimately obtained. The measurement of the diameter of the polymeric particles revealed that the particle diameter decreased from 2.4 to 1.4 and then to 0.9  $\mu\text{m}$  as the solvent

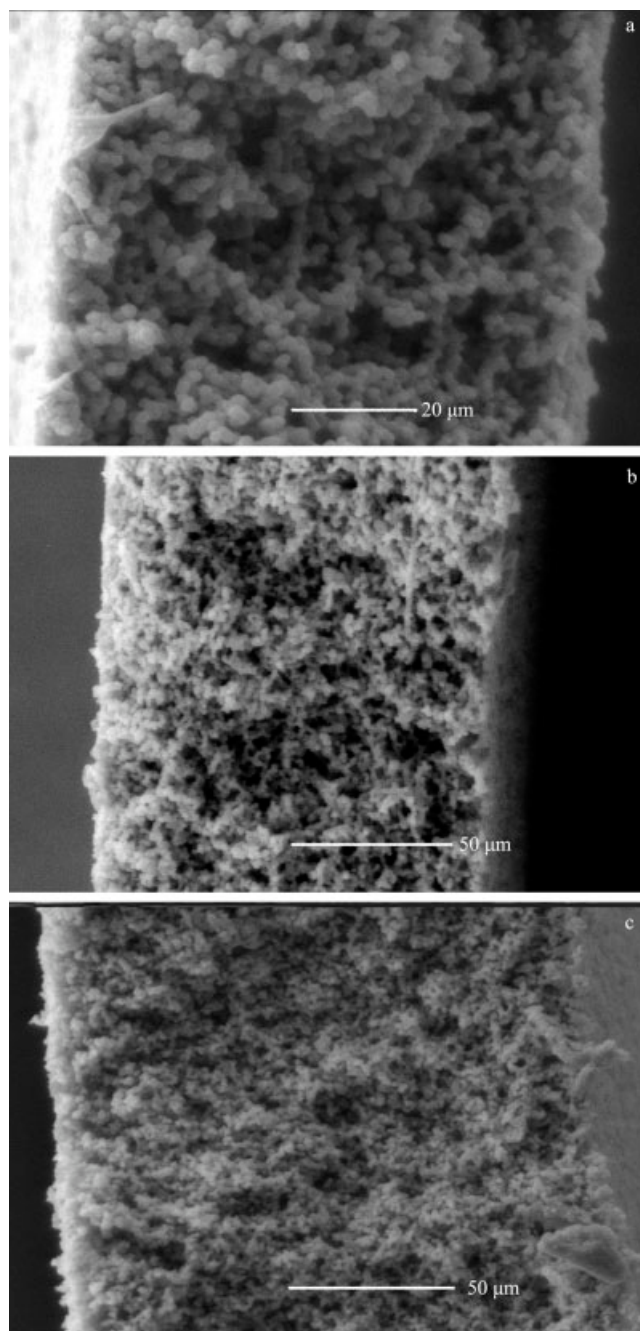


**Figure 3** Micrographs of EVA membranes cast from 5 wt % EVA/THF solutions at different preliminary drying times (casting thickness = 580  $\mu\text{m}$ ): (a) no preliminary drying time, (b) a preliminary drying time of 10 s, and (c) a preliminary drying time of 20 s.

evaporation period was increased from 0 to 10 and 20 s, respectively.

When the cast membrane immediately enters the coagulation bath, because of the quick solvent–non-solvent exchange, instantaneous phase inversion will take place, and the nuclei of the polymer-rich phase will form. Because the number of the nuclei is small and the growth of the polymer-rich phase continues around the limited number of nuclei, a large size but a smaller number of polymeric particles are produced. When the evaporation time is increased, a thicker boundary layer is formed at the coagulation media/polymer solution interface. This boundary layer will lower the solvent–nonsolvent exchange rate. Hence, the precipitation process is slowed, forming a larger number of new nuclei. This leads to the formation of a larger number of particles with smaller sizes.

### CONCLUSIONS

From the aforementioned observations, the following conclusions can be drawn:

1. The membrane becomes denser as the coagulation bath temperature increases.
2. The continuous phase is a polymer-rich phase when the film is cast from a 12 wt % EVA solution. The nuclei of the dilute phase migrate to the coagulation media/cast polymer solution interface and escape from the cast film when the cast film thickness is small. On the other hand, the nuclei of the dilute phase are captured in the continuous polymer-rich phase and macrovoids are formed in the ultimately obtained membrane when the cast film thickness is large.
3. The polymer-rich phase is dispersed in a continuous dilute phase when the film is cast from a 5 wt % EVA solution.
4. As the evaporation period increases, the number of nuclei of the polymer-rich phase increases, and the size of the nuclei decreases; this results in the decrease in the size of the polymer particles in the ultimately obtained membrane.
5. Because of the low nitrogen gas permeability in the membranes prepared at higher coagulation bath temperatures (39 and 53°C), they seem to be suitable for gas-separation applications, but the membranes prepared at lower coagulation bath temperatures (19 and 4°C) may be suitable for microfiltration, ultrafiltration, or both.

The authors are grateful to Takeshi Matsuura, Professor Emeritus of the University of Ottawa, for his kind assistance and supervision in this work.

### References

1. Cabasso, I. *Encyclopedia of Polymer Science and Engineering*; Wiley: New York, 1985; Vol. 9.
2. Weir, M. R.; Rutinduka, E.; Detellier, C.; Feng, C. Y.; Wang, Q.; Matsuura, T.; Le Van Mao, R. *J Membr Sci* 2001, 182, 41.
3. Chaturvedi, B. K.; Ghoshb, A. K.; Ramachandranb, V.; Trivedi, M. K.; Han Tab, M. S.; Misrab, B. M. *Desalination* 2001, 133, 31.
4. Cooper, A. R. *Ultrafiltration Membranes and Their Applications*; Plenum: New York, 1980.
5. Jones, C. D.; Fidalgo, M.; Wiesner, M. R.; Barron, A. R. *J Membr Sci* 2001, 193, 175.
6. Godjevargova, T.; Konsulov, V.; Dimov, A. *J Membr Sci* 1999, 152, 235.
7. Mahendran, R.; Malaisamy, R.; Arthanareeswaran, G.; Mohan, D. *J Appl Polym Sci* 2004, 6, 3659.
8. Sonnenschein Mark, F. *J Appl Polym Sci* 1999, 5, 1146.
9. Nouzaki, K.; Nagata, M.; Araib, J.; Idemotob, Y.; Kourab, N.; Yanagishita, H.; Negishi, H.; Kitamoto, D.; Ikegami, T.; Haraya, K. *Desalination* 2002, 144, 53.
10. Xu, Z.-L.; Qusayff, F. A. *J Appl Polym Sci* 2004, 5, 3398.
11. Deshmukh, S. P.; Li, K. *J Membr Sci* 1998, 150, 75.
12. Yang, S.; Liu, Z. *J Membr Sci* 2003, 222, 87.
13. Fromer, M. A.; Feiner, I.; Kedem, O.; Bloch, R. *Desalination* 1970, 7, 393.
14. Guillotin, M.; Lemoyne, C.; Noel, C.; Monnerie, L. *Desalination* 1977, 21, 165.
15. Strathman, H.; Kock, K. *Desalination* 1977, 21, 241.
16. Wijmans, J. G.; Kant, J.; Mulder, M. H. V.; Smolders, C. A. *Polymer* 1985, 26, 1539.
17. Marais, S.; Saiter, J. M.; Devallencourt, C.; Nguyen, Q. T.; Métayer, M. *Polym Test* 2002, 21, 425.
18. Mousavi, S. A.; Roostazad, R.; Ramazani, A. Presented at Macro 2004, Paris, France, July 2004.
19. Kesting, R. E. *Synthetic Polymeric Membranes*; McGraw-Hill: New York, 1991.
20. Mulder, M. H. V. *Basic Principles of Membrane Technology*; Kluwer Academic: Dordrecht, 1996.